Hindawi
Journal of Nanomaterials
Volume 2020, Article ID 8174871, 6 pages
https://doi.org/10.1155/2020/8174871

Research Article

Superparamagnetic Behaviour and Surface Analysis of Fe_3O_4/PPY/CNT Nanocomposites

Juniastel Rajagukguk,[1] **Pintor Simamora**,[1] **C. S. Saragih**,[1] **Hairus Abdullah**,[2] **Noto Susanto Gultom**,[1] **and Agung Imaduddin**[3]

[1]*Department of Physics, Faculty of Mathematics and Natural Sciences, Universitas Negeri Medan, 20221, Indonesia*
[2]*Department of Industrial Engineering, Universitas Prima Indonesia, Medan, Indonesia*
[3]*Research Center for Metallurgy of Materials, Indonesian Institute of Sciences, Serpong 15310, Indonesia*

Correspondence should be addressed to Juniastel Rajagukguk; juniastel@unimed.ac.id

Received 10 June 2020; Revised 25 September 2020; Accepted 7 October 2020; Published 22 October 2020

Academic Editor: Bhanu P. Singh

The superparamagnetic property of nanomaterials such as Fe_3O_4 has been considered to be promising for various applications. In this paper, Fe_3O_4/PPY/CNT nanocomposites were synthesized with utilizing natural iron sand by a coprecipitation method. The as-precipitated Fe_3O_4 NPs were combined with carbon nanotubes (CNTs) using conductive polypyrrole (PPY) as linking agents. The Fe_3O_4/PPY/CNT nanocomposites were systematically characterized by FE-SEM, EDS, XRD, BET, and FTIR. Furthermore, the effects of CNTs on magnetic and thermal properties of nanocomposites were investigated by VSM and thermal gravimetric analysis (TGA), respectively. The composites exhibited significant decrease of coercivity value with the content of CNTs increasing. The VSM result confirmed that Fe_3O_4/PPY/CNT nanocomposites were superparamagnetic. It was found that by increasing the amounts of CNTs, the magnetization of Fe_3O_4/PPY/CNT nanocomposites gradually decreased. The addition of CNTs is intended to improve the mesoporous property as proved by BET analysis which has the potential application as a nanocatalyst.

1. Introduction

Iron oxide is one of the most abundant metal oxides on the earth. There are four kinds of iron oxides such as magnetite, hematite, maghemite, and wüstite [1]. Among them, magnetite (Fe_3O_4) is the most studied due to its stability and wide range applications. The nanosized Fe_3O_4 has been used in several fields such as sensor, medical devise, drug delivery, data storage, and catalysts [2–6]. Superparamagnetism is an important property that is owned by Fe_3O_4 nanoparticles. Superparamagnetic Fe_3O_4 nanoparticles with a stable domain have anisotropy crystals that allow the reorientation and exchange of energy to easily produce hyperthermia magnetism. Superparamagnetic has the huge potential for various applications including magnetic resonance imaging (MRI), magnetic hyperthermia (MH), drug delivery, bioseparation, and biosensing [7–9].

One of the disadvantages of superparamagnetic Fe_3O_4 is being susceptible to agglomerate. A key strategy to overcome this issue is by adding polymers (e.g., PPY) during the preparation process. The usage of polymer not only can decrease particle size but also can improve the surface area and adsorption capability. Several studies have been developed to synthesize binary and ternary materials with Fe_3O_4 base

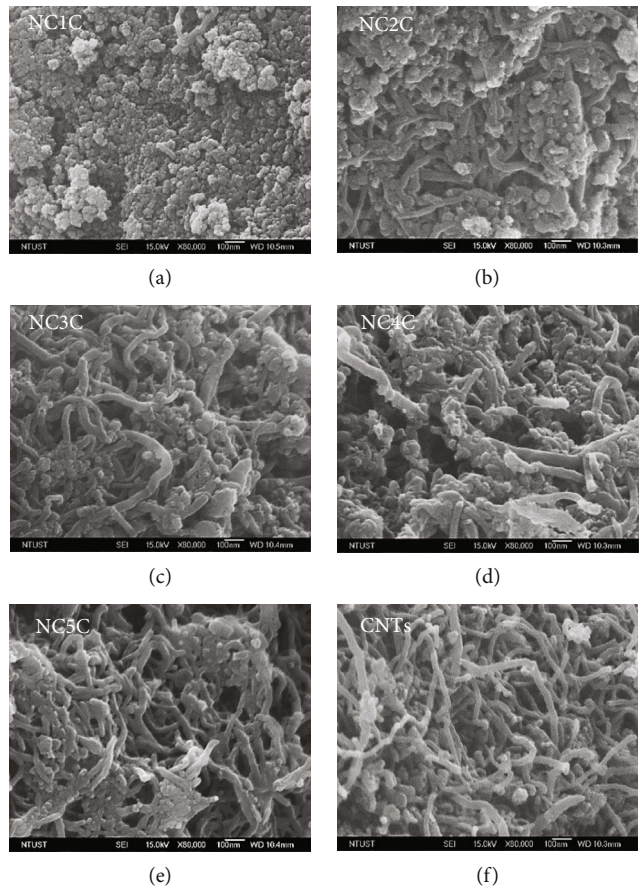

Figure 1: FE-SEM images of Fe_3O_4/PPY/CNT nanocomposites with (a) 0.5 g, (b) 1.5 g, (c) 2 g, (d) 2.5 g, (e) 3 g of CNTs, and (f) pure CNTs.

for different purposes. For example, Phadtare and coworkers designed Fe_3O_4/polymer composites for microwave-absorption applications [10]. Zhu et al. synthesized core shell Fe_3O_4/PANI for chromium reduction [11].

Carbon nanotubes (CNTs) have high modulus, high tensile strength, low density, and good electronic conductivity [12]. CNTs have attracted a great attention of scientists due to their unique structural, electrical, and mechanical properties. To improve the function of the ingredients, CNTs are supported by other materials to expand its applications. In an energy storage field, large numbers of ultrafine Fe_3O_4 nanoparticles covered on the surfaces of CNTs enhanced the electrochemical activity and mechanical property of the electrodes during the repeatedly charged and discharged processes and furthermore, the as-prepared CNT@Fe_3O_4 also exhibited mesoporous properties [13]. The hybrid structures are expected to improve electrochemical performance due to their unique structures, relative specific surface area, and high-porosity properties. The highly flexible and conductive CNT backbone provides a three-dimensional structure to facilitate electron transfer and provides a large contact area for higher Li^+ diffusion between electrodes and electrolytes [14].

In this contribution, we synthesize Fe_3O_4/PPY/CNTs with a low-cost and environmentally friendly coprecipitation method. Fe_3O_4 are coated with CNTs to enhance the properties of nanocomposites which are polymerized by polypyrrole (PPY). Furthermore, the effect of different amounts of CNT loading on the magnetic and surface properties is systematically investigated.

2. Experimental Sections

2.1. Materials. Natural iron sands were taken from Buaya River in Deli Serdang, North Sumatera. PPY was kindly received from Sigma-Aldrich. Hydrochloric acid (Merck 37%), ammonium solution (Merck 32%), and polyethylene glycol (PEG 6000) were purchased from Merck. Carbon nanotubes (CNTs) with a diameter of 25 nm were provided by Hanwha Chemical, Korea. Deionized (D.I.) water was used throughout the experiment for washing and neutralizing the pH.

2.2. Synthesis of Fe_3O_4 from Natural Iron Sand. The Fe_3O_4 nanoparticles were prepared by the coprecipitation method according to the following procedures. First, 10 grams of natural iron sand was dissolved into 250 ml HCl (12 M) solution under constant stirring of 300 rpm. After stirring for 90 min, the solution was filtered by using a filter paper. After that, 1 mmol of polyethylene glycol was added into iron filtrate. Under steady stirring, 200 ml ammonia (6.5 M) was wisely dropped into the solution and heated

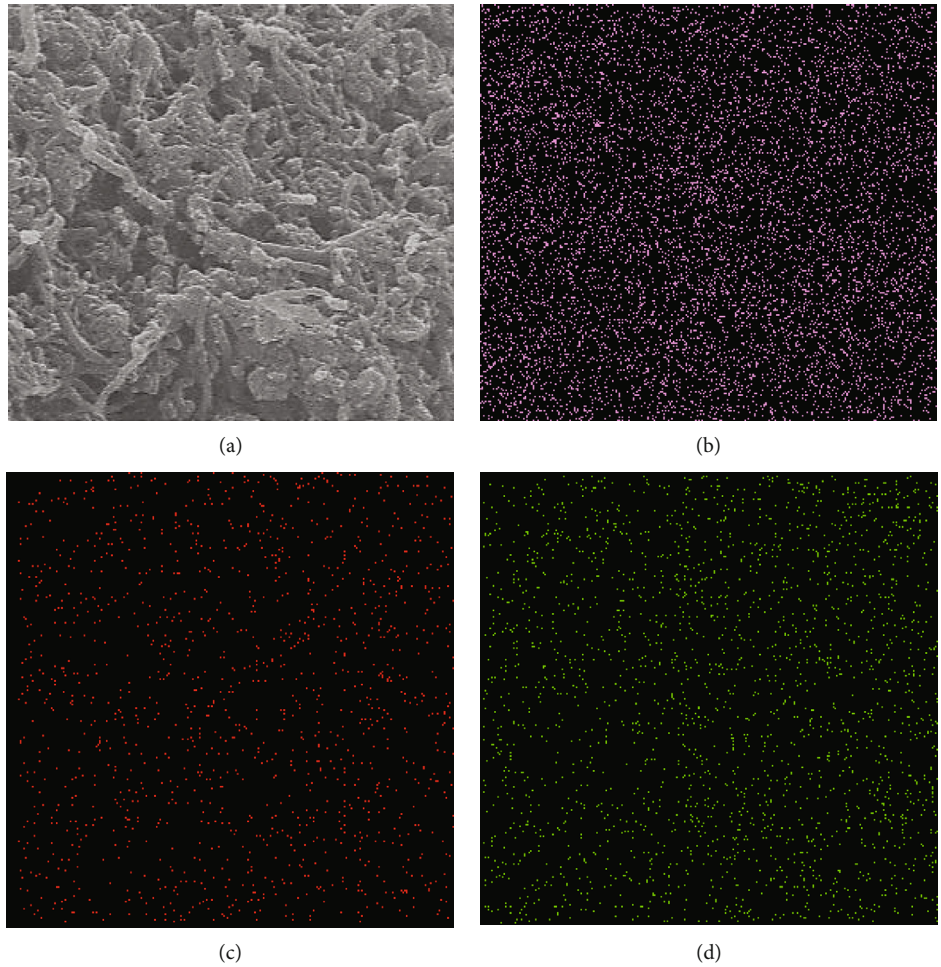

Figure 2: Elemental mapping of Fe_3O_4/PPY/CNT nanocomposites for the elements of (b) carbon, (c) iron, and (d) oxygen with the signals that were obtained from image (a).

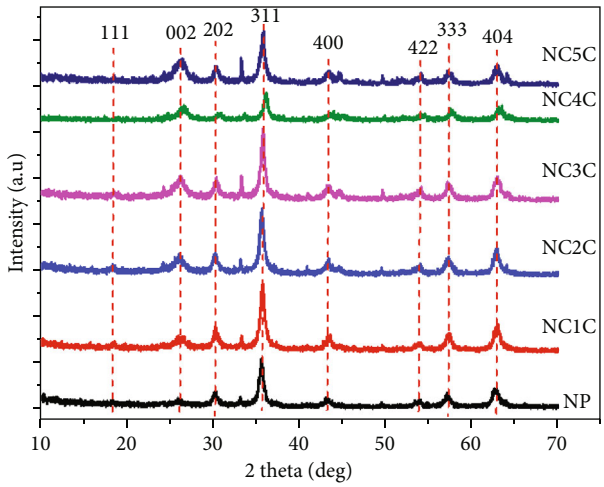

Figure 3: XRD pattern of Fe_3O_4/PPY/CNT nanocomposites.

at 70°C for another 90 min. The obtained precipitate was separated from the solution by centrifugation and washed repeatedly with D.I. water. Lastly, the Fe_3O_4 solid powders were dried in the oven at 100°C for 5 hours.

2.3. Synthesis of Fe_3O_4/PPY/CNT Nanocomposites. Fe_3O_4/PPY/CNT nanocomposites with different amounts of CNT were prepared by dispersing 5 g Fe_3O_4 and x g CNTs ($x = 0.5$, 1.5, 2.25, and 3 g, further denoted as NC1C, NC2C, NC3C, and NC4C, respectively) in the 300 ml D.I. water with ultrasonication for 1 h. After that, 10 g PPY was added into the above solution under constant stirring. The polymerization was initiated by adding $FeCl_3$ (66 g/l) as an oxidation agent. The solution was kept stirred at 0–5°C for 8 h. Finally, the obtained products were washed and dried in a vacuum oven overnight.

2.4. Characterizations. X-ray diffraction pattern of the samples was recorded by an X-ray diffractometer (Rigaku) with Cu-Kα ($\lambda = 1.54$ Å). The morphology of Fe_3O_4/PPY/CNT was observed using a field-emission scanning electron microscope (FE-SEM, JEOL 6500). The magnetization was measured using a vibrating sample magnetometer (VSM) MPMS 3. Brunauer–Emmett–Teller (BET, BEL JAPAN) was used to measure the surface area and absorption/desorption curve of the samples. The infrared spectra were recorded using Shimadzu 8201-FC. Thermogravimetry analysis (TGA,

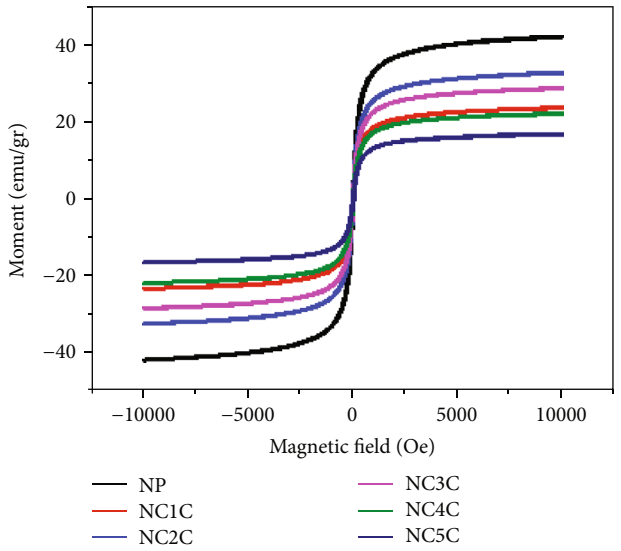

Figure 4: Vibrating sample magnetometer (VSM) analysis of Fe_3O_4/PPY/CNT nanocomposites.

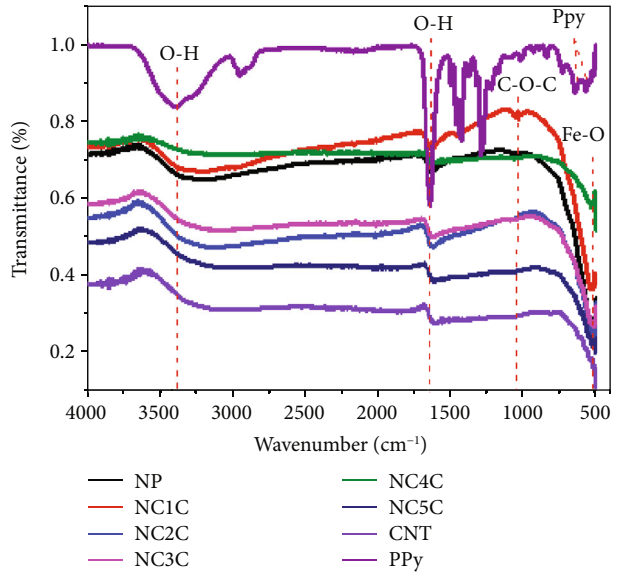

Figure 5: FTIR spectra of Fe_3O_4/PPY/CNT nanocomposites with different contents of CNTs.

TA Q500) was carried out to determine the thermal decomposition of Fe_3O_4/PPY/CNT.

3. Results and Discussion

The morphology of Fe_3O_4/PPY/CNT nanocomposites with different amounts of CNTs was observed by a field-emission scanning electron microscope (FE-SEM). As shown in Figure 1(a), Fe_3O_4 has a spherical shape with a particle size of 20–50 nm which is also similar to our previous work [15]. Figures 1(a)–1(e) show SEM images of Fe_3O_4/PPY/CNT nanocomposites with variations of CNT contents. The microstructure of pure CNTs is also shown in Figure 1(f) with a tube size less than 100 nm. It was observed that CNTs

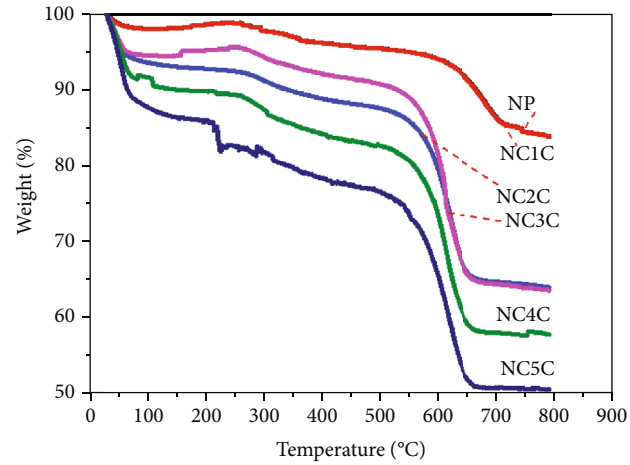

Figure 6: Thermal gravimetric analysis (TGA) of Fe_3O_4/PPY/CNT nanocomposites in nitrogen atmosphere.

were well deposited on the surfaces of Fe_3O_4 nanoparticle (NPs). As compared to the pure CNT without Fe_3O_4 NPs, the nanocomposites possibly have the Fe_3O_4 NPs penetrated inside the CNT to make its size larger.

FE-SEM equipped with an energy dispersive spectroscopy (EDS) analysis was further carried out to study the atomic composition of prepared samples. Figure 2 shows the EDS with elemental mapping of Fe_3O_4/PPY/CNT nanocomposite to show the presence of carbon, iron, and oxygen as indicated in Figures 2(b)–2(d). The contrast of elemental mapping showed that carbon was the major phase in the composites as compared to other elements, which was originated from CNT and PPY.

The XRD results of Fe_3O_4/PPY/CNT nanocomposite are shown in Figure 3. XRD patterns of as-prepared samples indicated that Fe_3O_4 phase had the cubic spinel crystal structure based on JCPDS card No. 19-0629. The main peaks of Fe_3O_4 located at 30.09, 35.20, 37.03, 43.05, 53.39, 56.94, and 62.51° for two theta correspond to crystal planes of (220), (311), (222), (400), (422), (511), and (440), respectively. The cubic structures of Fe_3O_4 were still clearly observed as the CNT amounts were increased. The crystallite size of the as-prepared samples was further estimated using the Scherrer equation [16]:

$$d = \frac{k\lambda}{B\cos\theta}, \quad (1)$$

where d is the crystallite size, k is a Scherrer constant, λ is the wavelength of X-ray, and B is the full width at half maximum (FWHM).

The calculated crystallite sizes of NP, NC1C, NC2C, NC3C, NC4C, and NC5C were 18.45, 18.26, 15.4, 18.28, 18.26, 18.96, and 19.77 nm, respectively. There was no significant change in the crystallite size for different amounts of CNTs.

The magnetic properties of Fe_3O_4/PPY/CNT nanocomposite were studied using vibrating-sample magnetometer. Figure 4 exhibits the magnetization of the as-prepared samples with different contents of CNTs. As there was no

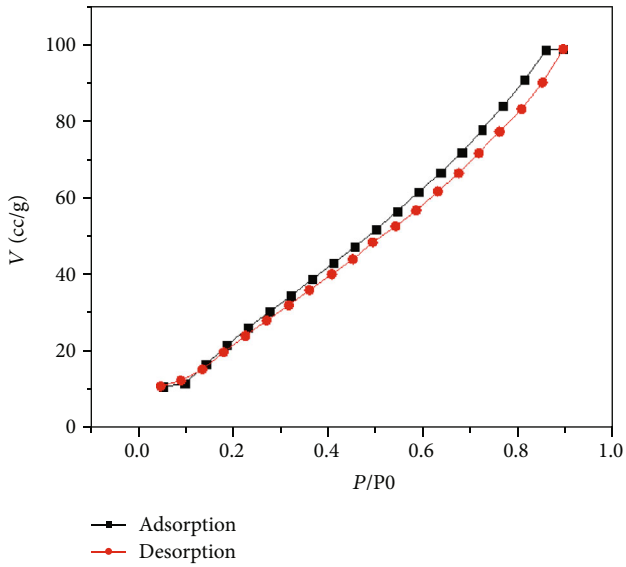

Figure 7: BET adsorption and desorption isotherm curve of the nanocomposite.

Table 1: BET analysis results of the as-prepared nanocomposites.

Samples	Surface area (m^2/g)	Pore volume (cc/g)	Pore size (nm)
NC1C	130.85	0.165	1.7393
NC2C	129.01	0.158	1.7404
NC3C	124.24	0.157	1.7405
NC4C	137.75	0.174	1.7409

hysteresis loop and coercivity was close to zero, the as-synthesized Fe_3O_4/PPY/CNT nanocomposites can be categorized as the superparamagnetic material. Without CNTs, Fe_3O_4 NPs had the highest saturation magnetization value of about 40 emu/gr. By increasing the content amounts of CNTs, the magnetization of Fe_3O_4/PPY/CNT nanocomposites gradually decreased. The lowest saturation magnetization was contributed by NC5C with a value of 15 emu/gr. The significant decreasing of magnetization is due to the existence of CNTs as nonmagnetic material that prevents the interaction between applied magnetic field and the intrinsic moments of Fe_3O_4 during the VSM measurements. The similar results were also found by Taufiq et al. where the magnetization of magnetite decreased from 30 to 9 emu/gr after the incorporation of silica [17]. Furthermore, due to the small coercivity value, Fe_3O_4/PPY/CNTs can be classified as a soft magnet material group.

Figure 5 displays the FTIR spectra of Fe_3O_4/PPY/CNT nanocomposites with different contents of CNTs. The peak at 570.2 cm^{-1} revealed Fe-O stretching. The presence of PPY was confirmed at 1072.42 cm^{-1} due to the C-O-C stretching [18]. The other peaks at 1627.9 and 3402.43 cm^{-1} were related to O-H bending and stretching bonds due to adsorbed water. Moreover, the results of FTIR also confirmed that PPY successfully interacted with nanocomposites as the correlation peak was shown at 1072.42 cm^{-1}.

Figure 6 indicates the thermogravimetry analysis of Fe_3O_4/PPY/CNT nanocomposites, which are examined from room temperature to 800°C in nitrogen atmosphere. The decrease of spectra for all samples at the temperatures below 100°C was related to the adsorbed water evaporation. The data indicated that more water was adsorbed on nanocomposites as the amount of CNTs increases. The sample weight began to decrease from a temperature range of 50°C for all samples. NC2C and NC3C samples experienced the same mass shrinkage which was around 30%. The samples of NC4C and NC5C indicated a mass shrinkage about 35% and 40%, respectively. The mass shrinkage is caused by the thermal decomposition of adsorbed organic substances and CNTs [19].

To investigate the surface area, pore size, and pore volume, BET analysis was conducted with absorption and desorption process. Figure 7 represents the BET nitrogen adsorption/desorption isotherm curve of the as-prepared NC4C nanocomposite. The isotherm curve closely matches to a typical type IV isotherm graph confirming the mesoporous property of the nanocomposite [20]. The BET analysis is conducted mainly to provide surface areas, pore sizes, and pore volumes of the as-prepared nanocomposites. The results of BET analysis are provided in Table 1. The NC4C sample had the largest surface area compared to the other samples. It can be concluded that the NC4C sample had a very small particle size compared to the others. Based on the BET analysis, it may be concluded that sample NC4C has a good adsorption property as compared to other samples.

4. Conclusions

Fe_3O_4/PPY/CNT nanocomposite has been successfully synthesized by the coprecipitation method. The XRD result indicated a cubic structure of the as-prepared Fe_3O_4 nanoparticles. The SEM analysis revealed that Fe_3O_4 nanoparticles were deposited on CNTs with a diameter of ~100 nm. FTIR of all samples showed that iron oxide and PPY were confirmed at 570.2 cm^{-1} and 1072.42 cm^{-1}, respectively. The BET isotherm curve closely matched to a typical type IV isotherm graph that confirms the mesoporous property of the as-prepared nanocomposites with high surface area of about 130 m^2/g. The VSM results confirmed that the as-prepared nanocomposite was superparamagnetic and had soft magnetic property. Based on the characterization results, the as-prepared Fe_3O_4/PPY/CNT nanocomposites are promising for many applications such as battery, as supercapacitor, and also as a substrate with a magnetic property to support catalyst development.

Data Availability

The data used to support the findings of this study are included within the article.

Conflicts of Interest

The authors declare that there are no conflicts of interest regarding the publication of this paper.

Acknowledgments

The first author would like to thank the Ministry of Science and Technology of the Republic of Indonesia for the grant Fundamental Research 2018-2019.

References

[1] J. Wollschläger, "Reactive molecular beam epitaxy of iron oxide films: strain, order, ansd interface properties," in *Encyclopedia of Interfacial Chemistry*, K. Wandelt, Ed., pp. 284–296, Elsevier, 2018.

[2] A. A. Asgharinezhad and H. Ebrahimzadeh, "Coextraction of acidic, basic and amphiprotic pollutants using multiwalled carbon nanotubes/magnetite nanoparticles@ polypyrrole composite," *Journal of Chromatography A*, vol. 1412, pp. 1–11, 2015.

[3] M. H. R. Zadeh, M. Seifi, H. Hekmatara, and M. B. Askari, "Preparation and study of the electrical, magnetic and thermal properties of Fe3O4 coated carbon nanotubes," *Chinese Journal of Physics*, vol. 55, no. 4, pp. 1319–1328, 2017.

[4] P. Simamora, C. S. Saragih, D. P. Hasibuan, and J. Rajagukguk, "Synthesis of nanoparticles Fe_3O_4/PEG/PPy-based on natural iron sand," *Materials Today: Proceedings*, vol. 5, no. 7, pp. 14970–14974, 2018.

[5] A. Suwattanamala, N. Bandis, K. Tedsree, and C. Issro, "Synthesis, characterization and adsorption properties of Fe_3O_4/MWCNT magnetic nanocomposites," *Materials Today: Proceedings*, vol. 4, no. 5, pp. 6567–6575, 2017.

[6] M. Tavakoli, F. Safa, and N. Abedinzadeh, "Binary nanocomposite of Fe3O4/MWCNTs for adsorption of Reactive Violet 2: Taguchi design, kinetics and equilibrium isotherms," *Fullerenes, Nanotubes, and Carbon Nanostructures*, vol. 27, no. 4, pp. 305–316, 2019.

[7] M. Montazer and T. Harifi, "Magnetic nanofinishes for textiles," in *Nanofinishing of Textile Materials*, M. Montazer and T. Harifi, Eds., pp. 225–240, Woodhead Publishing, 2018.

[8] A. Carvalho, A. R. Fernandes, and P. V. Baptista, "Chapter 10 - Nanoparticles as delivery systems in cancer therapy: focus on gold nanoparticles and drugs," in *Applications of Targeted Nano Drugs and Delivery Systems*, S. S. Mohapatra, Ed., pp. 257–295, Elsevier, 2019.

[9] T. D. Clemons, R. H. Kerr, and A. Joos, "Multifunctional magnetic nanoparticles: design, synthesis, and biomedical applications," in *Comprehensive Nanoscience and Nanotechnology (Second Edition)*, D. L. Andrews, R. H. Lipson, and T. Nann, Eds., pp. 193–210, Academic Press: Oxford, 2019.

[10] V. D. Phadtare, V. G. Parale, K. Y. Lee, T. Kim, V. R. Puri, and H. H. Park, "Flexible and lightweight Fe_3O_4/polymer foam composites for microwave-absorption applications," *Journal of Alloys and Compounds*, vol. 805, pp. 120–129, 2019.

[11] C. Zhu, F. Liu, L. Song, H. Jiang, and A. Li, "Magnetic Fe_3O_4@-polyaniline nanocomposites with a tunable core–shell structure for ultrafast microwave-energy-driven reduction of Cr(vi)," *Environmental Science: Nano*, vol. 5, no. 2, pp. 487–496, 2018.

[12] X. Zhang, W. Lu, G. Zhou, and Q. Li, "Understanding the mechanical and conductive properties of carbon nanotube fibers for smart electronics," *Advanced Materials*, vol. 32, no. 5, article 1902028, 2019.

[13] L. Fan, B. Li, N. Zhang, and K. Sun, "Carbon nanohorns carried iron fluoride nanocomposite with ultrahigh rate lithium ion storage properties," *Scientific Reports*, vol. 5, no. 1, 2015.

[14] G. Gao, Q. Zhang, X. B. Cheng et al., "Ultrafine ferroferric oxide nanoparticles embedded into mesoporous carbon nanotubes for lithium ion batteries," *Scientific Reports*, vol. 5, no. 1, 2015.

[15] E. A. Setiadi, S. S. Rahmat, M. Yunus et al., "The effect of synthesis temperature on physical and magnetic properties of manganese ferrite ($MnFe_2O_4$) based on natural iron sand," in *Journal of Physics: Conference Series, Volume 979, The 2nd International Conference on Science (ICOS)*, Makassar, Indonesia, 2017.

[16] Z. Xing, Q. Liu, A. M. Asiri, and X. Sun, "High-efficiency electrochemical hydrogen evolution catalyzed by tungsten phosphide submicroparticles," *ACS Catalysis*, vol. 5, no. 1, pp. 145–149, 2014.

[17] A. Taufiq, A. Nikmah, A. Hidayat et al., "Synthesis of magnetite/silica nanocomposites from natural sand to create a drug delivery vehicle," *Heliyon*, vol. 6, no. 4, article e03784, 2020.

[18] B. Mu, J. Tang, L. Zhang, and A. Wang, "*Facile fabrication of superparamagnetic graphene/polyaniline/Fe3O4 nanocomposites for fast magnetic separation and efficient removal of dye*," *Scientific Reports*, vol. 7, no. 1, p. 5347, 2017.

[19] Y. Tuo, G. Liu, B. Dong et al., "Microbial synthesis of Pd/Fe_3O_4, Au/Fe_3O_4 and $PdAu/Fe_3O_4$ nanocomposites for catalytic reduction of nitroaromatic compounds," *Scientific Reports*, vol. 5, no. 1, article 13515, 2015.

[20] G. Karunakaran, M. Kundu, G. Maduraiveeran et al., "*Hollow mesoporous heterostructures negative electrode comprised of CoFe2O4@ Fe3O4 for next generation lithium ion batteries*," *Microporous and Mesoporous Materials*, vol. 272, pp. 1–7, 2018.